CHEMICAL ENGINEERING TRANSACTIONS
VOL. 114, 2024

A publication of AIDIC
The Italian Association of Chemical Engineering
Online at www.cetjournal.it

Guest Editors: Petar S. Varbanov, Min Zeng, Yee Van Fan, Xuechao Wang

ISBN 979-12-81206-12-0; **ISSN** 2283-9216

DOI: 10.3303/CET24114040

The Sea-Based Waste Collection Routing Problem Using a Novel Value Recovery Function

Ricardo C. Alindayu II*, Jayne Lois G. San Juan, Charlle L. Sy

Industrial and Systems Engineering Department, De La Salle University, Philippines
ricardo_alindayu@dlsu.edu.ph

The Asia-Pacific region has been implicated as a major hotspot for plastic pollution in the world's oceans, causing environmental and economic damage to marine ecosystems and maritime industries. In response to this challenge, cleaning vessels have been optimized to collect floating plastic waste before retrieval becomes more costly and difficult. However, prior vessel routing optimization studies focused solely on cost minimization without considering the yield of collected plastic waste critical to the goal of plastic elimination from the oceans. As such, a mixed-integer linear programming model called the sea-based waste collection routing problem was developed to maximize value recovery through a novel profit function. Two computer-generated instances with differing node sizes were used to illustrate the functionalities of the SB-WCRP. A modified ant colony optimization algorithm was constructed to arrive at near-optimal solutions within a reasonable computing time given the problem's NP-hard nature. A benchmark with the branch-and-bound algorithm shows the modified ant colony optimization algorithm is suitable for large-case instances. Lastly, a sensitivity analysis on valuable fraction reveals the existence of a breakeven point that results in potential losses if not considered.

1. Introduction

The threat of marine plastics pollution continues to severely impact the Asia-Pacific region, with an estimated 650,000 Mt of plastic or around 65% of the global output emitted into the ocean per year (Meijer et al., 2021). This problem has resulted to around 10.8 billion USD worth of damages for the maritime industry (McIlgorm et al., 2022), and have been ingested by as much as 1,400 species of marine organisms eventually causing death (Monteiro et al., 2022). In response to this challenge, the United Nations Sustainable Development Goal 14 (Life Below Water) included the prevention and significant reduction of marine plastic pollution among its targets by 2025 (United Nations, 2015).

Among many interventions across the plastics value chain is the retrieval of plastic waste already existing in the environment before it causes any further damage (Richon et al., 2023). The collection of plastic waste combined with other interventions will further reduce leakage into the environment and ultimately approach zero over time (Tee and Sy, 2023). As such, the sea-based waste collection routing problem (SB-WCRP) was developed to optimize the routing of vessels in the clean-up of FPL from the ocean. The problem takes its roots from the vehicle routing problem; however, collection points move in space and time due to winds and ocean currents. Duan et al. (2020) presents a three-stage framework that resolves this constant motion. The first stage estimates locations and weights of floating plastic litter (FPL) hotspots using remote sensing data. The second stage predicts the motion of the identified FPL hotspots in the first stage using wind and current data. Time windows are assigned to each hotspot which represents the earliest and latest time a vessel can collect debris before it drifts too far away. Lastly, the third stage uses the parameters derived from the first two stages to arrive at an optimal collection route for the vessel.

Most of the models developed in the field focus solely on cost minimization as the main objective. The collection process involves the vessel traveling to various FPL hotspots and collecting debris within specified time windows, incurring fuel and operating costs, and finally returning to port to unload the debris, incurring fixed costs such as tugboat usage and dockage fees. Prior studies incorporate other kinds of costs such as additional fuel consumption from the weight of the vessel (Duan et al., 2021a) or the ocean currents (Duan et al., 2021b).

Paper Received: 27 June 2024; Revised: 18 July 2024; Accepted: 13 November 2024
Please cite this article as: Alindayu II R.C., San Juan J.L., Sy C.L., 2024, The Sea-Based Waste Collection Routing Problem Using a Novel Value Recovery Function, Chemical Engineering Transactions, 114, 235-240 DOI:10.3303/CET24114040

However, this paper argues that not only operational costs should be considered, but also the value recovery of waste. The value recovery is defined as the yield of plastic waste at the end of the collection period. This becomes especially critical to achieve the goal of zero plastics in the ocean (Jatinkumar Shah et al., 2018). Given the limitations of existing remote sensing technologies, there is a possibility that identified FPL hotspots may have a low valuable fraction, comprising of mostly natural debris. These are not valuable to a clean-up practitioner, as plastic waste is often targeted for its recyclability and high risks to the environment.
Hence, this paper presents the sea-based waste collection routing problem using a novel profit function that incorporates the waste value recovery of plastic. The system's value recovery is determined by subtracting operating costs from the value of the collected plastic waste. A negative value recovery indicates losses, while a positive value recovery indicates gains. Two instances of the problem are solved using a modified ant colony optimization algorithm. Lastly, insights are drawn to provide recommendations for future studies in the field.

2. Methods

2.1 Problem Statement and Model Formulation

Let directed graph $V = G(N, E)$ represent the network of the SB-WCRP. The starting and ending nodes refer to the port where the vessel departs and unloads collection of marine debris. The remaining nodes of the network refer to the locations of the FPL hotspots. The Nomenclature section details the sets and parameters, while Table 1 summarizes the decision variables.

Table 1: Decision variables for the SB-WCRP

Variable	Description	Type
x_{ij}	1 if the vessel traverses $(i,j) \in E$; 0 if otherwise	Binary
t_i^a	Arrival time at debris location $i \in N$ for the vessel	Continuous
Q_i^w	Cumulative weight on collection vessel at debris location $i \in N$	Continuous
t_i^p	Excess/deficit time at debris location $i \in N$	Continuous
q_i^p	Penalty weight at debris location $i \in N$	Continuous

Map coordinates are used for FPL locations. Since the earth is an ellipsoid, the Haversine formula is used to calculate distance between two points (see Eq(1)). The constant *R* is the equatorial radius (6378.137 km).

$$d_{ij} = 2Rarcsin\sqrt{\sin^2\left(\left(d_j^y - d_i^y\right)/2\right) + \cos\left(dy_j\right)\cos(dy_i)\sin^2((dx_j - dx_i)/2)} \quad (1)$$

The assumptions of the problem are outlined as follows: (1) clean-up time is linearly proportional to the plastic weight, (2) the effect of winds and waves on the vessel may be neglected, (3) plastic does not sink to the bottom during the collection period, and (4) linear cost penalties are applied upon failure to reach the FPL hotspot before the latest time, however, all debris are collected at the end of the period. A continuous MILP formulation is developed over the total planning period for marine debris collection as proposed by Duan et al. (2020).

$$\max OF = f^w \sum_{i \in E_2} \lambda q_i^w - \Big(\sum_{(i,j)\in E} \frac{f^s b^s dist_{ij} x_{ij}}{v^{ave}} + \sum_{(i,j)\in E_2 \cup E_3} f^c b^c t_i x_{ij} + \sum_{d \in N_3} \sum_{i \in N_1} (f^u)(ta_d + \frac{Q_n^w}{k_u} - ta_i) + f^b + f^u + f^d \Big) - f^p \sum_{i \in E_2 \cup E_3} q_i^p \quad (2)$$

$$\sum_{i \in N_1} \sum_{j \in N_2} x_{ij} = 1 \quad (3)$$

$$\sum_{j \in N_2 \cup N_3} x_{ij} = 1 \qquad \forall i \in N_2 \quad (4)$$

$$\sum_{j \in N_2 \cup N_3} x_{ij} = \sum_{j \in N_1 \cup N_2} x_{ji} \qquad \forall i \in N_2 \quad (5)$$

$$\sum_{i \in N_1} \sum_{j \in N_2} x_{ij} = \sum_{i \in N_2} \sum_{j \in N_3} x_{ij} \quad (6)$$

$$Q_i^w + q_j^w \leq Q_j^w + C^w\left(1 - x_{ij}\right) \quad \forall (i,j) \in E \tag{7}$$

$$q_i^w \leq Q_i^w \leq \sum_{i \in N_2} q_i^w \quad \forall i \in N_2 \tag{8}$$

$$Q_i^w = 0 \quad \forall i \in N_1 \tag{9}$$

$$b^s\left(\sum_{d \in N_3} ta_d - \sum_{i \in N_1} ta_i\right) + (b^c - b^s)\sum_{i \in N_2}\sum_{j \in N_2 \cup N_3} t_i x_{ij} + b^c \sum_{i \in N_2}\sum_{d \in N_3} t_d x_{id} \leq C^f \tag{10}$$

$$ta_i + \frac{dist_{ij}}{v^{ave}} \leq ta_j + M_{ij}\left(1 - x_{ij}\right) \quad \forall (i,j) \in E_1 \tag{11}$$

$$ta_i + t_i + \frac{dist_{ij}}{v^{ave}} \leq ta_j + M_{ij}\left(1 - x_{ij}\right) \quad \forall i \in N_2, \forall (i,j) \in E_2 \cup E_3 \tag{12}$$

$$t_i^p = t_i^l - ta_i \tag{13}$$

$$q_i^p \geq -t_i^p \tag{14}$$

$$x_{ij} \in \{0,1\} \quad \forall (i,j) \in E \tag{15}$$

$$ta_i, Q_i^w, t_i^p, q_i^p \geq 0 \quad \forall i \in V \tag{16}$$

The objective function maximizes the total value recovery of the collection process as seen in Eq(2). The first term refers to the value of collected marine debris. The second term refers to the usage costs, and the fixed costs of berthing, unloading, and tugboat use. The last term refers to any penalty costs if the vessel violates any time windows. (Eq)3 to (Eq)6 describe the flow continuity constraints of the vessel. Eq(7) describes the cumulative weight of the vessel as it collects debris from point to point. Eq(8) assures that collected debris does not exceed the actual debris on the ground. Eq(9) initializes the collection at the origin port to zero. Eq(10) limits operations to the fuel capacity of the vessel. Eq(11) and Eq(12) calculate the arrival time of the vessel. Eq(13) and Eq(14) present the penalty function. Lastly, Eq(15) and Eq(16) describe the binary and continuous variables of the model, respectively.

2.2 Modified Ant Colony Optimization Algorithm

A modified ant colony optimization (mACO) algorithm is developed given the problem's NP-hard nature to arrive at near-optimal solutions within a reasonable amount of time (Islam and Rahman, 2012). This becomes particularly relevant when node sizes increase, and exact methods take significantly long to arrive at solutions. The branch-and-bound (B&B) algorithm is used to benchmark the mACO algorithm to illustrate the efficiency of the latter for higher node sizes. Both algorithms were implemented on MATLAB2024a with a MacBook Air M1 chip.

2.2.1 Set Initial Parameters and Create New Ant Colony

The number of iterations n, ants $k \in K$, initial pheromone matrix τ, and desirability function η are set to start the loop. The ants randomly select a closed-loop pathway, where selection of the next node follows a probability function p_k detailed in Eq(17). The relative importance of the pheromone α and relative importance of the fitness function β quantify the bias of ants selecting the next node.

$$p_k(i,j) = \begin{cases} \dfrac{\left[\tau_{ij}\right]^\alpha \left[\eta_{ij}\right]^\beta}{\sum \left[\tau_{ij}\right]^\alpha \left[\eta_{ij}\right]^\beta} \\ 0, if\ otherwise \end{cases} \tag{17}$$

2.2.2 Calculate the Fitness Values of the Ant Colony

After each ant selects a route, the fitness value is calculated accordingly. A conditional fitness function is described in Eq(18). If the arrival time exceeds the time window, then a cost penalty is added to the fitness function. However, if the time window is satisfied, then no penalty is incurred. The ant with the best fitness function is the optimal solution for this iteration but is improved with updating the pheromone matrix.

$$\eta_{ij} = \begin{cases} f^w \lambda q_i^w - \left[\frac{f^s b^s dist_{ij} x_{ij}}{v^{ave}} + f^c b^c t_i x_{ij} + (f^u)(ta_d + t_d - ta_i)\right] - f^p q_i^p, if\ ta_i < t_i^e\ or\ ta_i > t_i^l \\ f^w \lambda q_i^w - \left[\frac{f^s b^s dist_{ij} x_{ij}}{v^{ave}} + f^c b^c t_i x_{ij} + (f^u)(ta_d + t_d - ta_i)\right], \quad if\ otherwise \end{cases} \tag{18}$$

2.2.3 Update Pheromone Matrix

The pheromone matrix is reduced by evaporation using rate ρ. Afterwards, the fitness values for each ant in the colony are added to update the pheromone matrix for this iteration in Eq(19). A new colony is generated again to repeat the process until all iterations are completed and the solution converges.

$$\tau_{ij}^k = (1-\rho)\tau_{ij} + \sum_{k=1}^{m} \Delta\tau_{ij}^k \tag{19}$$

2.3 Model and Algorithm Parameters

Two instances of varying node sizes are developed to illustrate the model's functionality and the mACO algorithm's performance. The node sizes were selected based on prior calculations, where a drastic change in computing time was measured when six nodes were increased to seven. As such, the small instance was set at six nodes, while the large instance was set at twelve nodes. The instances (Table 2) and the vessel and algorithm parameters (Table 3) were either generated or derived from prior studies (Duan et al., 2020).

Table 2: Small and large instances (LN – longitude in decimal, LT – latitude in decimal, M – mass in kg, V – volume in m^3, ET – earliest time in hh:mm, LT – latest time in hh:mm)

	Small instance						Large instance					
Node	LN	LT	M	V	ET	LT	LN	LT	M	V	ET	LT
Port	120.942	14.632	-	-	8:00	18:00	120.942	14.632	-	-	8:00	18:00
1	120.906	14.648	184.242	0.196	8:00	13:00	120.802	14.584	33.508	0.035	8:00	13:00
2	120.849	14.641	44.291	0.047	8:00	13:00	120.728	14.655	134.947	0.143	8:00	13:00
3	120.867	14.653	60.949	0.064	8:00	12:00	120.752	14.539	136.411	0.145	8:00	12:00
4	120.848	14.603	144.900	0.154	8:00	17:00	120.875	14.525	140.396	0.149	8:00	17:00
5	120.930	14.608	92.485	0.098	8:00	16:00	120.833	14.694	53.473	0.057	8:00	16:00
6	120.899	14.627	222.340	0.236	8:00	11:00	120.776	14.594	702.587	0.748	8:00	11:00
7	-	-	-	-	-	-	120.725	14.523	37.268	0.039	8:00	13:00
8	-	-	-	-	-	-	120.695	14.652	629.182	0.670	8:00	13:00
9	-	-	-	-	-	-	120.940	14.568	209.847	0.223	8:00	12:00
10	-	-	-	-	-	-	120.889	14.514	59.178	0.063	8:00	17:00
11	-	-	-	-	-	-	120.807	14.732	43.352	0.046	8:00	16:00
12	-	-	-	-	-	-	120.837	14.601	36.261	0.038	8:00	11:00

Table 3: Model and algorithm parameters

Variable	Value	Variable	Value	Variable	Value	Variable	Value
f^b	14 USD/hr	f^u	90 USD	b^c	30 L/hr	n	1000
f^d	7.5 USD	v^{ave}	15.465 km/hr	b^s	50 L/hr	k	300
f^t	450 USD	C^w	10000 kg	f^c	1.5 USD/L	ρ	0.85
f^w	50 USD/kg	C^f	10000 L	f^s	3 USD/L	α	1
f_i^e	50 USD/hr	k_c	180 kg/hr	λ	1	β	1
f_i^p	50 USD/hr	k_u	300 kg/hr				

3. Results and Discussion

Table 4 highlights the best profits and routes of the small and large instances. The best profit refers to the optimal profit calculated by the value recovery function. The route details the order of the vessel from the port to the nodes and ending at the port in a closed loop. Two algorithm performance indicators are also summarized in Table 4 to quantify algorithm performance. The Optimality Gap column refers to the percent difference of the calculated solution with the optimal solution. The Time column refers to the computing time to arrive at the solution to evaluate the algorithm's performance. For the small instance, both the mACO and B&B algorithms have comparable performance, by converging at the same route and best profit with the same optimality gap and time. However, the computing time of the mACO algorithm for the small instance is approximately 63 times longer than the B&B algorithm, revealing that exact methods may be more ideal for lower node sizes. For the large instance, the use of the mACO converges to a near-optimal solution with an optimality gap of 6.03%, which is greater than the optimality gap of the B&B algorithm. Despite this, the mACO arrives at a solution within a reasonable amount of time compared to the exact solution which takes approximately 60 times longer. Hence, the mACO can be used to arrive at near-optimal solutions in a reasonable amount of time for large instances of the problem. Exact methods to arrive at the optimal solution may take too long for incremental increases in profit that may not be significant for the decision maker, which in this case is only 1.5% less than the result of B&B.

Table 4: Instance solutions and benchmarking results

	mACO Algorithm			B&B Algorithm		
Instance	Best Profit (USD)	Optimality Gap (%)	Time (s)	Best Profit (USD)	Optimality Gap (%)	Time (s)
Small	35,294	0.19	82.09	35,294	0.19	1.31
	Route: Port → 6 → 1 → 3 → 2 → 4 → 5 → Port			Route: Port → 6 → 1 → 3 → 2 → 4 → 5 → Port		
Large	101,610	6.03	87.38	103,170	4.27	5344.14
	Route: Port → 10 → 9 → 4 → 5 → 11 → 8 → 2 → 7 → 3 → 1 → 12 → 6 → Port			Route: Port → 9 → 10 → 4 → 12 → 1 → 7 → 3 → 6 → 2 → 8 → 11 → 5 → Port		

Figure 1 illustrates a sensitivity analysis for the small instance by altering the fraction of valuable waste in the FPL hotspot λ. The nominal values for weight in Table 2 assume that all collected debris are composed completely of plastic. This is not a realistic case as quantified by the valuable fraction measured at the end of the collection period. When the valuable fraction decreases, the profit decreases up to a breakeven point of 0.05784 where the cleaning operation results in losses. This relation holds true for the assumed value of waste at 50 USD/kg, but losses are expected at higher valuable fractions for lower waste values. As such, decision makers can decide whether to implement the clean-up operations if the predicted fraction of valuable waste is expected to result in gains or losses depending on the plastic pollution load or if the market for recyclable plastic waste is very positive.

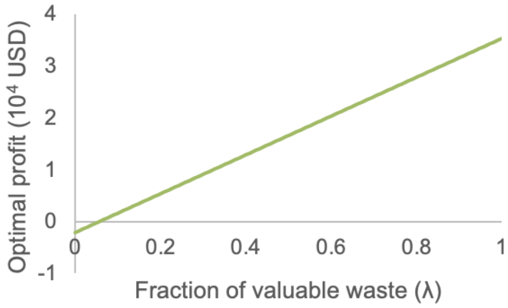

Figure 1: Change in profit of the small instance after change in fraction of valuable waste.

4. Conclusions

The SB-WCRP developed in this paper is the first to utilize the value recovery of plastic waste for clean-up operations in the ocean, balancing plastic recovery with fixed and operational costs. On a practical note, the value recovery function can provide decision makers an idea whether the collection should push through depending on the conditions that cause the operations to breakeven, as seen in the results. The small instance resulted in a profit of 35,294 USD with an optimality gap of 0.19%, while the large instance resulted in a profit of 101,610 USD with an optimality gap of 6.03%. For the small case study instance, a breakeven point of 0.0578 valuable fraction was calculated, meaning the operations would be profitable if at least 5.78% of the FPL hotspots were composed of plastic. A modified ant colony optimization algorithm was developed to arrive at near-optimal solutions within a reasonable amount of time especially for large case instances, converging 60-times faster than exact methods. This comes at the cost of sacrificing incremental profit, however, this may be insignificant to a decision maker with a 1.5% decrease in the large instance case study. On the other hand, exact methods such as the B&B algorithm can be used for small case instances given faster convergence while guaranteeing the optimality of solutions. The following recommendations are provided for future studies of the SB-WCRP: (1) consider the uncertainty in model parameters by adopting a stochastic or robust optimization approach, (2) consider a fleet of vessels to reduce penalty costs, and lastly, (3) consider other metaheuristic algorithms that may converge more efficiently compared to the ant colony optimization algorithm.

Nomenclature

N_1 – Set of the origin port, $\{0\}$
N_2 – Set of predicted locations of MPP hotspots, $\{1,2,\ldots,n\}$
N_3 – Set of the destination port, $\{n+1\}$
N – Set of all nodes, $N_1 \cup N_2 \cup N_3$
E_1 – Set of all edges that connect the origin harbor to the predicted MPP hotspots, $\{(i,j)|i \in N_1, j \in N_2\}$
E_2 – Set of all edges that connect the predicted MPP hotspots to other MPP hotspots, $\{(i,j)|i,j \in N_2, i \neq j\}$
E_3 – Set of all edges that connect the predicted MPP hotspots to the destination harbor, $\{(i,j)|i \in N_2, j \in N_3\}$
E – Set of all edges, $E_1 \cup E_2 \cup E_3$
t_i – Collection time at debris location $i \in N_2$
t_d – Berth time at destination harbor $d \in N_3$
f^b – Berth cost at destination harbor $d \in N_3$
f^d – Dockage cost at destination harbor $d \in N_3$
f^t – Tugboat cost at destination harbor $d \in N_3$
f^w - Revenue for each kilogram of collected debris
f_i^e – Penalty cost per hour from earliest time window
f_i^p – Penalty cost per hour from latest possible time
$[t_i^e, t_i^l]$ – Time window of debris location $i \in N_2$
f^u - Hourly usage cost of collection vessel
v^{ave} - Average sailing velocity of collection vessel
C^w - Weight capacity of collection vessel
C^f - Fuel tank capacity of collection vessel
d_{ij} – Length of edge $(i,j) \in E$
b^c - Hourly fuel consumption of collection vessel during collection or berth at destination harbor
b^s - Hourly fuel consumption of collection vessel during sailing
f^c - Hourly fuel cost of collection vessel during collection or berth at destination harbor
f^s - Hourly fuel cost of collection vessel during sailing
λ - Fraction of valuable waste in FPL hotspot

References

Duan G., Nur F., Alizadeh M., Chen L., Marufuzzaman M., Ma J., 2020, Vessel routing and optimization for marine debris collection with consideration of carbon cap. Journal of Cleaner Production, 263, 121399.

Duan G., Fan T., Chen X., Chen L., Ma J., 2021a, A hybrid algorithm on the vessel routing optimization for marine debris collection. Expert Systems with Applications, *182*, 115198.

Duan G., Aghalari A., Chen L., Marufuzzaman M., Ma J., 2021b, Vessel routing optimization for floating macro-marine debris collection in the ocean considering dynamic velocity and direction. Transportation Research Part E: Logistics and Transportation Review, 152, 102414.

Islam R., Rahman M. S., 2012, An ant colony optimization algorithm for waste collection vehicle routing with time windows, driver rest period and multiple disposal facilities. 2012 International Conference on Informatics, Electronics & Vision (ICIEV), 774–779.

Jatinkumar Shah P., Anagnostopoulos T., Zaslavsky A., Behdad S., 2018, A stochastic optimization framework for planning of waste collection and value recovery operations in smart and sustainable cities. Waste Management, 78, 104–114.

McIlgorm A., Raubenheimer K., McIlgorm D. E., Nichols R., 2022, The cost of marine litter damage to the global marine economy: Insights from the Asia-Pacific into prevention and the cost of inaction. Marine Pollution Bulletin, 174, 113167.

Meijer L. J. J., van Emmerik T., van der Ent R., Schmidt C., Lebreton L., 2021, More than 1000 rivers account for 80% of global riverine plastic emissions into the ocean. Science Advances, 7(18), eaaz5803.

Monteiro R., Andrades R., Noleto-Filho E., Pegado T., Morais L., Gonçalves M., Santos R., Sbrana A., Franceschini S., Soares M. O., Russo T., Giarrizzo T., 2022, GLOVE: The Global Plastic Ingestion Initiative for a cleaner world. Marine Pollution Bulletin, *185*, 114244.

Richon C., Kvale K., Lebreton L., Egger M., 2023, Legacy oceanic plastic pollution must be addressed to mitigate possible long-term ecological impacts. Microplastics and Nanoplastics, *3*(1), 25.

Tee M., Sy C., 2023, A Simulation Model to Analyze the Efficacy of Plastic Waste Management Policies, Chemical Engineering Transactions, 103, 1-6.

United Nations. (2015). Transforming our world: The 2030 Agenda for Sustainable Development.